Journal of Magnetism and Magnetic Materials 456 (2018) 423–432

Contents lists available at ScienceDirect

Journal of Magnetism and Magnetic Materials

journal homepage: www.elsevier.com/locate/jmmm

Research articles

Exact expression for the magnetic field of a finite cylinder with arbitrary uniform magnetization

Alessio Caciagli [1], Roel J. Baars [1], Albert P. Philipse, Bonny W.M. Kuipers *

Van 't Hoff Laboratory for Physical and Colloid Chemistry, Debye Institute for Nanomaterials Science, Utrecht University, Padualaan 8, 3584 CH Utrecht, The Netherlands

ARTICLE INFO

Article history:
Received 3 November 2017
Received in revised form 29 January 2018
Accepted 1 February 2018

Keywords:
Electromagnetic fields
Magnetism
Elliptic integrals
Electromagnetic theory
Finite element method

ABSTRACT

An exact analytical expression for the magnetic field of a cylinder of finite length with a uniform, transverse magnetization is derived. Together with known expressions for the magnetic field due to longitudinal magnetization, the calculation of magnetic fields for cylinders with an arbitrary magnetization direction is possible. The expression for transverse magnetization is validated successfully against the well-known limits of an infinitely long cylinder, the field on the axis of the cylinder and in the far field limit. Comparison with a numerical finite-element method displays good agreement, making the advantage of an analytical method over grid-based methods evident.

1. Introduction

Analytic expressions for the magnetic fields produced by inherently magnetic materials or induced in magnetically susceptible materials, are only well-known for some classic textbook cases, such as the field of point multipoles and infinitely long wires carrying a current [1–4]. In the past, many papers on demagnetization factors [5–11] and cylindrical ferromagnets [12–15] have been published. In demagnetization tensors with regard to uniformly magnetized finite cylinders, implicit analytic expressions have been incorporated [16,17]. Kraus [16] applies a magnetic surface charge method using integrals that contain Bessel functions. Tandon et al. [17] and Beleggia et al. [18,19] employ a Fourier transform approach. Herein use is made of a shape function that is equal to the trace of the demagnetization tensor, which connection is difficult to derive from the commonly used magnetic surface charge description. Magnetic fields of complex geometries often can be solved only numerically via finite element methods (F.E.M.) [20,21]. However, the domain discretization inherent to these methods may ultimately lead to numerical inaccuracies, unless expensive higher-order calculations are performed, or the calculation mesh is refined. The analytic modelling of the field has a clear advantage over finite-element methods as the necessary magnetic quantities can be probed at all required coordinates, with minimal computational effort. This is highly useful, for example, when dynamical systems are modelled, such as the movement of magnetic nanoparticles in magnetic field gradient [22,23].

A geometry for which analytical expressions for magnetic quantities are readily available, is an axisymmetric solenoid of finite length [24–27]. Exact expressions for the vector potential $\mathbf{\Phi}$, magnetic flux density $\mathbf{B}$ (with axial and radial components), magnetic force $\mathbf{F} = (\mathbf{m} \cdot \nabla)\mathbf{B}$, where $\mathbf{m}$ is the magnetic dipole moment of the object, and other quantities can be formulated using special functions such as elliptic integrals. The derivation of these expressions usually extends the treatment of a single circular current loop by integrating over a certain length along the symmetry axis of the loop [28,29]. The solenoid field also describes the field of a cylindrical uniform permanent magnet with its magnetization vector $\mathbf{M}$ along the axis of symmetry (longitudinal magnetization). For different magnetization directions, such as $\mathbf{M}$ perpendicular to the axis of symmetry (transverse magnetization), other field equations are required. In the case of transverse magnetization, explicit analytical results are available for an infinite cylinder [2,30], and for the on-axis field of a finite cylinder derived by Wysin [31]. To expand upon these known relations, we have derived an explicit, analytical expression for the magnetic field of a transversely, uniformly magnetized finite cylinder in all spatial field points, inside as well as outside the cylinder. By combining the expression for longitudinal and transverse magnetization we will also demonstrate the possibility of accurately calculating the resulting magnetic field for a cylinder with an arbitrarily chosen magnetization vector.

* Corresponding author.
E-mail address: b.w.m.kuipers@uu.nl (B.W.M. Kuipers).
[1] Both authors contributed equally to this work.

https://doi.org/10.1016/j.jmmm.2018.02.003
0304-8853/

The expressions derived here are applied to the modelling of a high-gradient magnetic separation process, using a separation filter comprising many small magnetizable fibres. By combining the local magnetic fields of a large collection of (non-overlapping) cylinders, we aim to calculate the movement of magnetic nanoparticles through such a separation filter [32] and whether, ultimately, the nanoparticles can be trapped by the filter. In this paper, in addition to the calculations for a single cylinder, we explore the possibility to calculate the magnetic field for a combination of multiple cylinders by means of our analytical expressions, which is also relevant for a broad range of other applications [33–35].

2. Preliminary

Consider a circular cylindrical body of radius R and semi-length L, with its centroid at the origin of a cylindrical coordinate system (ρ, φ, z) and its axis aligned with the z-direction (see Fig. 1). A uniform magnetization of the body along an arbitrarily chosen magnetization vector $\mathbf{M}$ can always be decomposed into a longitudinal and transverse component,

$$\mathbf{M} = M_{\mathrm{l}}\hat{\mathbf{z}} + M_{\mathrm{t}}\hat{\rho} \tag{1}$$

In reality, for a magnetizable material, the acquired magnetization will in general not have the same direction as the applied field $\mathbf{H}_{\mathrm{ext}}$, as the magnetization vector will rotate to minimize its energy depending on the magnetic susceptibility of the material and the demagnetization factors of the body. The Stoner-Wohlfarth model describes this principle in detail [36,37]. In general, the magnetization is related to the magnetic field $\mathbf{H}$, the magnetic flux density $\mathbf{B}$ and the permeability of vacuum μ_0 through,

$$\mathbf{B} = \mu_0(\mathbf{H} + \mathbf{M}) \tag{2}$$

We proceed by restating the known expression for $\mathbf{B}$ for longitudinal magnetization [25,27] and continue by deriving an expression for the case of transverse magnetization. The validity of the equations are tested by determining several limiting cases. By combining Eqs. (1) and (2), the field of a finite cylinder with an off-axis magnetization vector is calculated and these results are compared with numerical calculations. Finally, the applicability of our model to the description of magnetizable cylinders are tested against the results of a finite element method.

3. Longitudinal magnetization (review of past work)

Equations for the field inside and outside a longitudinally magnetized, finite cylinder were first retrieved by Callaghan and Maslen [25]. They obtained their result by considering a finite cylinder as a collection of current loops (i.e. an ideal solenoid). The total magnetization is $M \equiv nI$, with n the number of turns per unit of length and I the current per turn. By applying the Biot–Savart law, the magnetic field can be calculated directly in terms of elliptic integrals. Derby and Olbert [27] revisited the derivation and provided a computationally convenient form using a combination of generalized complete elliptic integrals [38]. They correctly retrieved the field of a current loop in the limit $L \to 0$ and the far-field limit of a point dipole at large distances from the cylinder.

In Derby and Olbert [27] only an integral form of the field equations is given. Here we restate these results in closed form, in terms of elliptic integrals, obtaining equations similar to those for the transverse case presented in the following section.

$$\begin{aligned} B_\rho &= \frac{\mu_0 MR}{\pi}\left[\alpha_+ P_1(k_+) - \alpha_- P_1(k_-)\right] \\ B_z &= \frac{\mu_0 MR}{\pi(\rho+R)}\left[\beta_+ P_2(k_+) - \beta_- P_2(k_-)\right] \end{aligned} \tag{3}$$

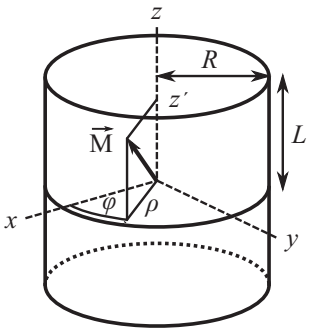

Fig. 1. Schematic representation of a magnetized cylinder of semi-length L and radius R with an arbitrary magnetization vector $\mathbf{M}$. The cylindrical (ρ, φ, z), and Cartesian (x, y, z) coordinate systems are indicated.

where B_ρ and B_z are the radial and axial components of the magnetic flux density, respectively. Two auxiliary functions are defined (see Appendix A) as,

$$\begin{aligned} P_1(k) &= \mathcal{K} - \frac{2}{1-k^2}(\mathcal{K} - \mathcal{E}) \\ P_2(k) &= -\frac{\gamma}{1-\gamma^2}(\mathcal{P} - \mathcal{K}) - \frac{1}{1-\gamma^2}\left(\gamma^2\mathcal{P} - \mathcal{K}\right) \end{aligned} \tag{4}$$

and the following shorthand notations will be employed:

$$\begin{aligned} \xi_\pm &= z \pm L & & \\ \alpha_\pm &= \tfrac{1}{\sqrt{\xi_\pm^2 + (\rho+R)^2}} & \beta_\pm &= \xi_\pm \alpha_\pm \\ \gamma &= \frac{\rho - R}{\rho + R} & k_\pm^2 &= \frac{\xi_\pm^2 + (\rho-R)^2}{\xi_\pm^2 + (\rho+R)^2} \end{aligned} \tag{5}$$

The symbols $\mathcal{K}$, $\mathcal{E}$ and $\mathcal{P}$ are used to indicate the evaluation of the complete elliptic integrals of the first, second and third kind, as follows,

$$\begin{aligned} \mathcal{K} &= \mathrm{K}\left(\sqrt{1-k^2}\right) &&= \int_0^{\frac{\pi}{2}} \tfrac{\mathrm{d}\theta}{\sqrt{1-(1-k^2)\sin^2\theta}} \\ \mathcal{E} &= \mathrm{E}\left(\sqrt{1-k^2}\right) &&= \int_0^{\frac{\pi}{2}} \mathrm{d}\theta \sqrt{1-(1-k^2)\sin^2\theta} \\ \mathcal{P} &= \Pi\left(1-\gamma^2, \sqrt{1-k^2}\right) &&= \int_0^{\frac{\pi}{2}} \tfrac{\mathrm{d}\theta}{\left(1-(1-\gamma^2)\sin^2\theta\right)\sqrt{1-(1-k^2)\sin^2\theta}} \end{aligned} \tag{6}$$

Note that B_φ is absent in Eq. (3) due to the radial symmetry of the system. A visualization of the magnetic field lines produced by these equations is given in Fig. 2a.

4. Transverse magnetization

To derive the field equations for a transversely magnetized cylinder, we follow the approach of Callaghan and Maslen [25] and Derby and Olbert [27]. We start by choosing a magnetization vector perpendicular to the long axis of the cylinder. A convenient choice is a magnetization along the Cartesian x-axis, $\mathbf{M} = M\hat{\mathbf{x}}$, although any direction in the xy-plane would be suitable for symmetry reasons. Assuming there are no free currents present, the magnetic field can be expressed as the gradient of a magnetostatic scalar potential

$$\mathbf{H} = -\nabla\Phi_{\mathrm{m}} \tag{7}$$

In the following, we derive the exact expression for the potential Φ_{m}. The components of the $\mathbf{H}$-field can be derived following similar mathematical manipulations, but only the final results will be presented in Section 4.2.

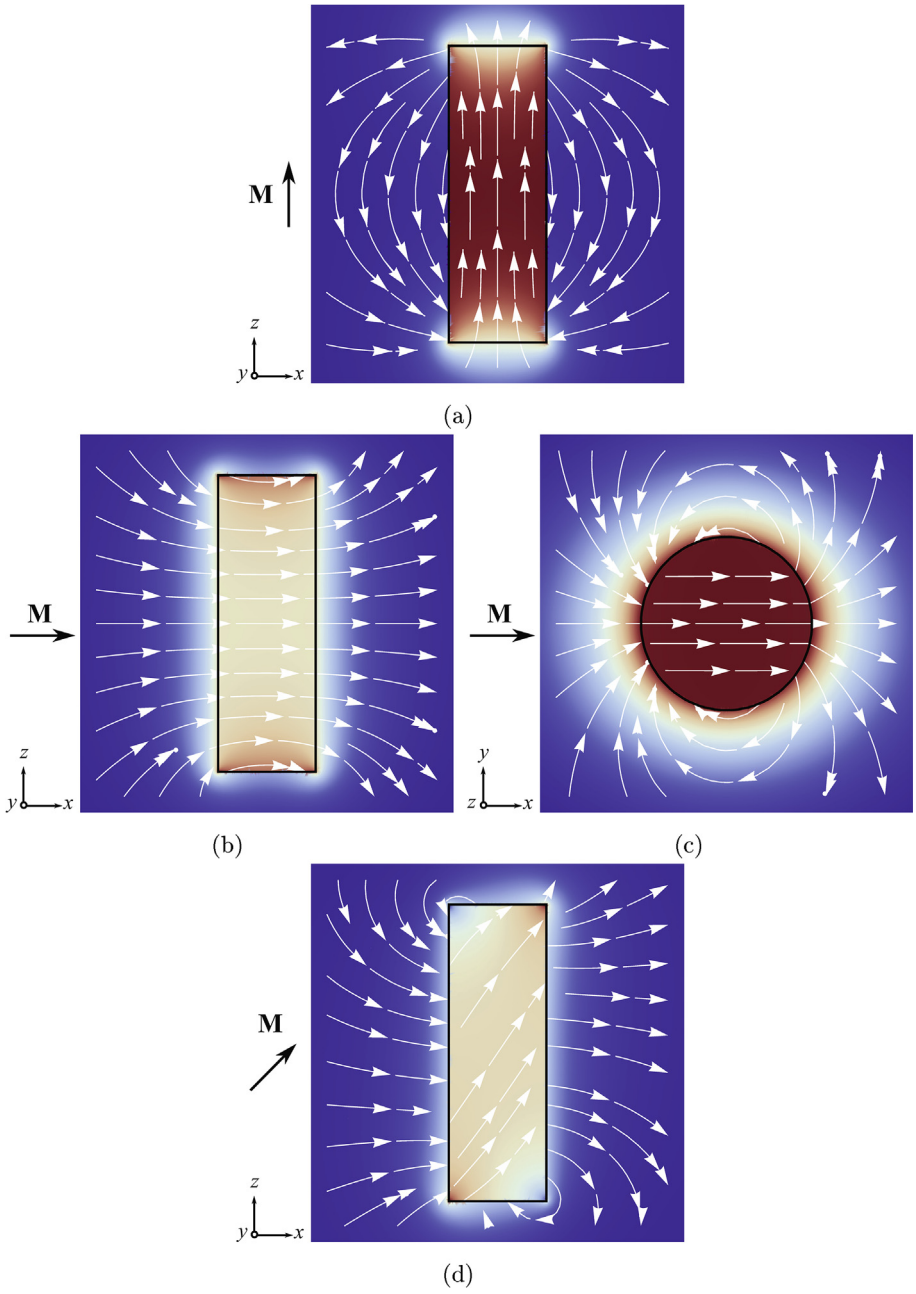

Fig. 2. Magnetic flux lines and density plots for a cylinder ($R = 1$, $L = 3$) with longitudinal (a), transverse (b) and (c), and off-axis magnetization (d). The outline of the cylinder is marked with a black rectangle or circle. The colours indicate the magnitude of the B-field strength (blue = low, red = high).

4.1. Magnetostatic potential

In general, the magnetostatic potential at a point $\mathbf{r}$ can be written as [2],

$$\Phi(\mathbf{r}) = \int_V \mathrm{d}\mathbf{r}' \, \frac{\rho(\mathbf{r}')}{4\pi|\mathbf{r}-\mathbf{r}'|} \tag{8}$$

using the bound magnetic charge formulation, where $\rho(\mathbf{r}')$ is the volume charge density. One may recognize Green's function for the Laplacian, $G(\mathbf{r}) = (4\pi|\mathbf{r}|)^{-1}$. In the problem of interest, the volume charge density reduces to a surface charge distribution σ on the lateral surface of the cylinder. In cylindrical coordinates this is given by $\sigma(\varphi') = M\cos\varphi'$. The integral in Eq. (8) is now reduced to an integral over the surface of the cylinder,

$$\Phi(\rho,\varphi,z) = \frac{M}{4\pi}\int_0^{2\pi}\mathrm{d}\varphi' \int_{-L}^{L}\mathrm{d}z' \, \frac{R\cos\varphi'}{\sqrt{\rho^2+R^2-2\rho R\cos(\varphi-\varphi')+(z-z')^2}} \tag{9}$$

We proceed by evaluating the above integral in several steps, to a functional form containing elliptic integrals. First, the integral over z' is evaluated, giving,

$$\frac{MR}{4\pi}\int_0^{2\pi}\mathrm{d}\varphi' \cos\varphi' \ln\left(\xi+\sqrt{\xi^2+\rho^2+R^2-2\rho R\cos(\varphi-\varphi')}\right)\Bigg|_{\xi_-}^{\xi_+} \tag{10}$$

where the substitution $\xi_\pm = z \pm L$ from Eq. (5) is introduced.

Integration by parts can be applied, leading to the somewhat involved expression,

$$\frac{MR}{4\pi}\left\{\left[\sin\varphi'\ln\left(\xi+\sqrt{\xi^2+\rho^2+R^2-2\rho R\cos(\varphi-\varphi')}\right)\right|_{\xi_-}^{\xi_+}\Bigg|_{\varphi'=0}^{\varphi'=2\pi}\right] + \int_0^{2\pi}\mathrm{d}\varphi'\,\sin\varphi'\left[\frac{\rho R\sin(\varphi-\varphi')}{\sqrt{\xi^2+\rho^2+R^2-2\rho R\cos(\varphi-\varphi')}} \times\frac{1}{\xi+\sqrt{\xi^2+\rho^2+R^2-2\rho R\cos(\varphi-\varphi')}}\Bigg|_{\xi_-}^{\xi_+}\right]\right\} \tag{11}$$

Evaluation of the first term between square brackets shows that it vanishes. The remainder can be rewritten to,

$$-\frac{M\rho R^2}{4\pi}\int_0^{2\pi}\mathrm{d}\varphi'\,\sin\varphi'\left[\frac{\sin(\varphi-\varphi')}{\rho^2+R^2-2\rho R\cos(\varphi-\varphi')} \times\frac{\xi}{\sqrt{\xi^2+\rho^2+R^2-2\rho R\cos(\varphi-\varphi')}}\Bigg|_{\xi_-}^{\xi_+}\right] \tag{12}$$

The integral over φ' is solved by two consecutive changes in integration variable. First, $2\psi=\pi-(\varphi-\varphi')$, resulting in,

$$-\frac{M\rho R^2}{\pi}\int_{\frac{\pi}{2}-\frac{\varphi}{2}}^{\frac{3}{2}\pi-\frac{\varphi}{2}}\mathrm{d}\psi\left(\sin\varphi(\sin^2\psi-\cos^2\psi)-2\cos\varphi\sin\psi\cos\psi\right) \times\frac{\cos\psi\sin\psi}{\rho^2+R^2-2\rho R(\sin^2\psi-\cos^2\psi)}\frac{\xi}{\sqrt{\xi^2+\rho^2+R^2-2\rho R(\sin^2\psi-\cos^2\psi)}}\Bigg|_{\xi_-}^{\xi_+} \tag{13}$$

where $\sin\varphi'$, $\sin(\varphi-\varphi')$ and $\cos(\varphi-\varphi')$ have been evaluated in terms of basic trigonometric functions. It can be shown that the first term between the larger parentheses does not contribute to the integral, leaving,

$$\frac{2M\rho R^2\cos\varphi}{\pi}\int_{\frac{\pi}{2}-\frac{\varphi}{2}}^{\frac{3}{2}\pi-\frac{\varphi}{2}}\mathrm{d}\psi\,\frac{\cos^2\psi\sin^2\psi}{\rho^2+R^2-2\rho R(\sin^2\psi-\cos^2\psi)} \times\frac{\xi}{\sqrt{\xi^2+\rho^2+R^2-2\rho R(\sin^2\psi-\cos^2\psi)}}\Bigg|_{\xi_-}^{\xi_+} \tag{14}$$

Making use of the shorthand from Eq. (5) and applying a second change in variable, $\sin\psi=x$, allows us to write,

$$\begin{aligned}\rho^2+R^2-2\rho R(\sin^2\psi-\cos^2\psi)&=(\rho+R)^2\left(1-x^2(1-\gamma^2)\right)\\ \xi_\pm^2+\rho^2+R^2-2\rho R(\sin^2\psi-\cos^2\psi)&=\left(\xi_\pm^2+(\rho+R)^2\right)\left(1-x^2(1-k_\pm^2)\right)\end{aligned} \tag{15}$$

which upon substitution into Eq. (14) leads to,

$$\frac{2M\rho R^2\cos\varphi}{\pi(\rho+R)^2}\int_{-\cos\frac{\varphi}{2}}^{\cos\frac{\varphi}{2}}\mathrm{d}x\,\frac{(1-x^2)x^2}{1-x^2(1-\gamma^2)}\frac{\beta_\pm}{\sqrt{(1-x^2)\left(1-x^2\left(1-k_\pm^2\right)\right)}}\Bigg|_{\xi_-}^{\xi_+} \tag{16}$$

Note the additional factor $1/\sqrt{1-x^2}$ entering the expression because of the change of variable. A more convenient form of this integral is found by applying the following substitution,

$$\frac{(1-x^2)x^2}{1-x^2(1-\gamma^2)}=\frac{1}{1-\gamma^2}\left(\frac{\gamma^2}{1-\gamma^2}+x^2-\frac{\gamma^2}{1-\gamma^2}\frac{1}{1-x^2(1-\gamma^2)}\right) \tag{17}$$

Splitting the integral in Eq. (16) according to the terms in Eq. (17), gives three separate integrals representing (combinations of) elliptic integrals of the first, second and third kind.

The full expression now becomes,

$$\frac{2M\rho R^2\cos\varphi}{\pi(\rho+R)^2(1-\gamma^2)}\left(\frac{\gamma^2}{1-\gamma^2}\int_{-\cos\frac{\varphi}{2}}^{\cos\frac{\varphi}{2}}\mathrm{d}x\frac{\beta_\pm}{\sqrt{(1-x^2)\left(1-x^2\left(1-k_\pm^2\right)\right)}}\Bigg|_{\xi_-}^{\xi_+} + \int_{-\cos\frac{\varphi}{2}}^{\cos\frac{\varphi}{2}}\mathrm{d}x x^2\frac{\beta_\pm}{\sqrt{(1-x^2)\left(1-x^2\left(1-k_\pm^2\right)\right)}}\Bigg|_{\xi_-}^{\xi_+} - \frac{\gamma^2}{1-\gamma^2}\int_{-\cos\frac{\varphi}{2}}^{\cos\frac{\varphi}{2}}\mathrm{d}x\frac{1}{1-x^2(1-\gamma^2)}\frac{\beta_\pm}{\sqrt{(1-x^2)\left(1-x^2\left(1-k_\pm^2\right)\right)}}\Bigg|_{\xi_-}^{\xi_+}\right) \tag{18}$$

Each term can be evaluated using tabulated integrals (cf. Ref. [39]). After some elementary rewriting, a concise final result is obtained,

$$\Phi=\frac{MR\cos\varphi}{\pi}\left[\beta_+P_3(k_+)-\beta_-P_3(k_-)\right] \tag{19}$$

where we define the auxiliary function $P_3(k)$ as,

$$P_3(k)=\frac{1}{1-k^2}(\mathcal{K}-\mathcal{E})-\frac{\gamma^2}{1-\gamma^2}(\mathcal{P}-\mathcal{K}) \tag{20}$$

4.2. Magnetic field

To obtain expressions for the magnetic field components in Eq. (7), the derivatives of the scalar potential Φ in Eq. (19) can be taken directly. Alternatively, the derivatives can be taken in Eq. (9), followed by a similar mathematical treatment as was used for the scalar potential. For brevity, only the final expressions are presented here:

$$\begin{aligned}H_\rho&=-\frac{\partial\Phi}{\partial\rho}&&=\frac{MR\cos\varphi}{2\pi\rho}\left[\beta_+P_4(k_+)-\beta_-P_4(k_-)\right]\\ H_\varphi&=-\frac{1}{\rho}\frac{\partial\Phi}{\partial\varphi}&&=\frac{MR\sin\varphi}{\pi\rho}\left[\beta_+P_3(k_+)-\beta_-P_3(k_-)\right]\\ H_z&=-\frac{\partial\Phi}{\partial z}&&=\frac{MR\cos\varphi}{\pi}\left[\alpha_+P_1(k_+)-\alpha_-P_1(k_-)\right]\end{aligned} \tag{21}$$

where an auxiliary function P_4 is defined as,

$$P_4(k)=\frac{\gamma}{1-\gamma^2}(\mathcal{P}-\mathcal{K})+\frac{\gamma}{1-\gamma^2}\left(\gamma^2\mathcal{P}-\mathcal{K}\right)-P_1(k) \tag{22}$$

Computational effort in the evaluation of these equations is minimal, because of the availability of efficient algorithms to calculate elliptical integrals [40–42]. Fig. 2b and c show a graphical representation of the field lines for a cylinder with transverse magnetization.

Note that analytical expressions for the derivatives of Eq. (21) can be derived easily. This enables the calculation of magnetic forces through $\mathbf{F}=(\mathbf{m}\cdot\nabla)\mathbf{B}$ for all points in space, except on the cylinder surface edge. Forces are typically required when performing molecular dynamics (MD) modeling, such as Brownian dynamics simulations of nanoparticles [32].

4.3. Combined action of orthogonal magnetization components

Knowing the magnetic field equations for a cylinder with fully longitudinal and transverse magnetization (Eqs. (3) and (21)),

allows the calculation of the field also for intermediate magnetizations. By decomposing the total magnetization in its longitudinal and transverse contributions according to Eq. (1), the magnetic field for an off-axis magnetization direction is calculated. For the magnetization direction $\mathbf{M} = (1/\sqrt{2}, 0, 1/\sqrt{2})$, the resulting field is shown in Fig. 2d.

5. Limiting cases

In this section we evaluate some limiting cases for the transversely magnetized cylinder, Eq. (21), and compare these with known expressions from literature. For a treatment of the limiting cases for a longitudinally magnetized cylinder see for example Callaghan and Maslen [25].

5.1. Infinite cylinder

In the limit of an infinite cylinder, $L \to \infty$, we have $k = 1$ and $\beta_\pm = \pm 1$. This simplifies the auxiliary functions for the radial and angular components in Eq. (21) to,

$$\begin{aligned}\left[\beta_+ P_4(\kappa_+) - \beta_- P_4(\kappa_-)\right] &= \pi \frac{1+\gamma^2-2\sqrt{\gamma^2}}{1-\gamma^2}\frac{\gamma}{\sqrt{\gamma^2}} \\ \left[\beta_+ P_3(\kappa_+) - \beta_- P_3(\kappa_-)\right] &= \frac{\pi}{2}\frac{1+\gamma^2-2\sqrt{\gamma^2}}{1-\gamma^2}\end{aligned} \tag{23}$$

The z-component correctly vanishes when evaluating the limits. These expressions contain a square root term accounting for points outside ($\gamma > 0$) and inside ($\gamma < 0$) the cylinder. Substitution of Eqs. (23) into (21) gives for the radial and angular component, after some rewriting,

$$H_\rho = \begin{cases} \frac{M}{2}\frac{R^2}{\rho^2}\cos\varphi, & \gamma > 0 \\ -\frac{M}{2}\cos\varphi, & \gamma < 0 \end{cases} \quad H_\varphi = \begin{cases} \frac{M}{2}\frac{R^2}{\rho^2}\sin\varphi, & \gamma > 0 \\ \frac{M}{2}\sin\varphi, & \gamma < 0 \end{cases} \tag{24}$$

which are identical to the known expressions from classical magnetostatics [2,30].

5.2. Field on axis

The magnetic field along the axis of the cylinder is found by evaluating Eq. (21) in the limit of $\rho \to 0$ and $\varphi = 0$. No angular or z-component will be present. In this case we have $\beta_\pm = \xi_\pm/\sqrt{(\xi_\pm^2 + R^2)}$, $\cos\varphi = 1$ and the elliptic integrals $\mathcal{K} = \mathcal{E} = \mathcal{P} = \pi/2$, so that $P_4(k) = -\frac{\pi}{2}(1+\gamma)/(1-\gamma)$. We can write,

$$H_\rho(0,0,z) = -\frac{MR}{4\rho}\frac{1+\gamma}{1-\gamma}\left(\frac{\xi_+}{\sqrt{\xi_+^2+R^2}} - \frac{\xi_-}{\sqrt{\xi_-^2+R^2}}\right) \tag{25}$$

The term $R/\rho(1+\gamma)/(1-\gamma)$ equals unity so that now the same expression is obtained as in [31],

$$H_\rho(0,0,z) = -\frac{M}{4}\left(\frac{\xi_+}{\sqrt{\xi_+^2+R^2}} - \frac{\xi_-}{\sqrt{\xi_-^2+R^2}}\right) \tag{26}$$

Evaluating the field in the origin $z = 0$ gives,

$$H_\rho(0,0,0) = -\frac{M}{2}\frac{L}{\sqrt{R^2+L^2}} = \begin{cases} -\frac{M}{2} & \text{if } L \gg R \\ -\frac{ML}{2R} & \text{if } L \ll R \end{cases} \tag{27}$$

again in agreement with earlier findings [31].

5.3. Far field limit

For the field far away from the cylinder, $\rho, z \gg R, L$, the field of a point dipole should be retrieved. The far-field limit is identical to the limit of $R, L \to 0$. We can arbitrarily set $\varphi = 0$ to eliminate the angular dependence through $\sin\varphi = 0$. To obtain the field equations, we make a first order series expansion around $L = 0$, followed by an additional expansion around $R = 0$. It is impractical to perform these expansions on the final results in Eq. (21) directly. We therefore start by considering the partial derivatives $H_\rho = -\partial\Phi/\partial\rho$ and $H_z = -\partial\Phi/\partial z$ in integral form (see Eq. (21), coming from Eq. (9)). For the radial component we have,

$$\frac{MR}{4\pi}\int_0^{2\pi} \mathrm{d}\varphi' \cos\varphi' \frac{\rho - R\cos\varphi'}{\rho^2+R^2-2R\rho\cos\varphi'} \frac{\xi}{\sqrt{\xi^2+\rho^2+R^2-2\rho R\cos\varphi'}}\Bigg|_{\xi_-}^{\xi_+} \tag{28}$$

The first order expansion of the argument of the integral around $L = 0$ gives,

$$\frac{MRL}{2\pi}\int_0^{2\pi} \mathrm{d}\varphi' \cos\varphi' \frac{\rho - R\cos\varphi'}{\left(z^2+\rho^2+R^2-2R\rho\cos\varphi'\right)^{3/2}} \tag{29}$$

Performing a consecutive expansion around $R = 0$ results in,

$$\frac{MRL}{2\pi}\int_0^{2\pi} \mathrm{d}\varphi' \left(\frac{\rho\cos\varphi'}{(z^2+\rho^2)^{3/2}} - \frac{R(z^2-2\rho^2)\cos^2\varphi'}{(z^2+\rho^2)^{5/2}}\right) \tag{30}$$

Evaluation of the integral eliminates the first term. Solving the remaining integral immediately leads to the final results for the radial component,

$$H_\rho = \frac{MR^2L}{2}\frac{2\rho^2-z^2}{(z^2+\rho^2)^{5/2}} \tag{31}$$

For the z-component, we follow similar steps, starting with,

$$-\frac{MR}{4\pi}\int_0^{2\pi} \mathrm{d}\varphi' \cos\varphi' \frac{1}{\sqrt{\xi^2+\rho^2+R^2-2\rho R\cos\varphi'}}\Bigg|_{\xi_-}^{\xi_+} \tag{32}$$

where the expansion around $L = 0$ leads to,

$$\frac{MRL}{2\pi}\int_0^{2\pi} \mathrm{d}\varphi' \cos\varphi' \frac{z}{\left(z^2+\rho^2+R^2-2\rho R\cos\varphi'\right)^{3/2}} \tag{33}$$

The second expansion around $R = 0$ gives,

$$-\frac{MRL}{2\pi}\int_0^{2\pi} \mathrm{d}\varphi' \left(\frac{z\cos\varphi'}{(z^2+\rho^2)^{3/2}} + \frac{3z\rho R\cos^2\varphi'}{(z^2+\rho^2)^{5/2}}\right) \tag{34}$$

As before, the first term in the integral cancels out, so that the final solution is given by,

$$H_z = \frac{MR^2L}{2}\frac{3\rho z}{(z^2+\rho^2)^{5/2}} \tag{35}$$

Eqs. (31) and (35) match the field for a point dipole [27], where only the radial and z variable are swapped because the alignment of the magnetization vector here is along the x-axis and not the z-axis.

6. The demagnetization tensor of a cylinder

6.1. Introduction

For a uniformly magnetized sample of arbitrary geometry, the demagnetization tensor is defined as [43,44]:

$$\mathbf{H}(\mathbf{r}) = -\mathbf{N}^P(\mathbf{r}) \cdot \mathbf{M} \tag{36}$$

where $\mathbf{M}$ is the uniform magnetization vector, $\mathbf{H}$ is the magnetic field (also known as the *demagnetizing field*), $\mathbf{r} = (x, y, z)$ is the point loca-

tion and $\mathbf{N}^P$ is the demagnetization tensor. In the general case $\mathbf{H}$ is non-uniform (here illustrated by its dependence on $\mathbf{r}$) and $\mathbf{N}^P$ as defined above is also known as the *point-function demagnetization tensor*. Its volume average defines the *magnetometric demagnetization tensor* [44]:

$$\langle \mathbf{H}(\mathbf{r}) \rangle_V = -\mathbf{N}^M \cdot \mathbf{M} \tag{37}$$

where $\langle \dots \rangle_V$ denotes the average over the sample volume and $\mathbf{N}^M$ is the magnetometric demagnetization tensor. Clearly, it follows that:

$$\mathbf{N}^M = \frac{1}{V} \int_V dV\, \mathbf{N}^P \tag{38}$$

Both the point-function and magnetometric demagnetization tensor $\mathbf{N}$ possess notable properties, such as unitary trace ($Tr(\mathbf{N}) = 1$) and symmetry ($\mathbf{N}_{ij} = \mathbf{N}_{ji}$ for $i \neq j$) [44]. Additionally, due to their symmetric nature, the tensors can always be diagonalized by choosing a suitable base. In particular, the principal values of the diagonalized $\mathbf{N}^M$ (which correspond to its eigenvalues) are known as the *magnetometric demagnetization factors*.

In the following we will derive the demagnetization tensors $\mathbf{N}^P$ and $\mathbf{N}^M$ as well as the demagnetization factors of a circular cylinder on the basis of the exact analytical expression of the demagnetizing field $\mathbf{H}$ for said geometry.

6.2. The point-function demagnetization tensor

Consider the uniform magnetization to be alternatively in the orthogonal x, y and z directions. Then $\mathbf{M} = M\hat{j}$ where $j = x, y, z$. From its definition, it follows that:

$$H_i(\mathbf{r}) = -N^P_{ij} M \tag{39}$$

with $i, j = x, y, z$. H_i denotes the component of $\mathbf{H}$ in the $\hat{\imath}$ direction due to the magnetization $\mathbf{M} = M\hat{j}$. Inverting the previous relation gives the value of the tensor elements as a function of the field $\mathbf{H}$. These are uniquely determined by the relation:

$$N^P_{ij} = -\frac{1}{M} H_i \quad \mathbf{M} = M\hat{j} \qquad i, j = x, y, z \tag{40}$$

in which the magnetization condition for each relation is reported. The relations can be expressed analytically by inserting the values of H_x, H_y and H_z as obtained when discussing the longitudinal and transverse magnetization cases, with the coordinate transformations:

$$H_x(x, y, z) = H_\rho(\rho, \varphi, z)\cos\varphi - H_\varphi(\rho, \varphi, z)\sin\varphi \tag{41}$$
$$H_y(x, y, z) = H_\rho(\rho, \varphi, z)\sin\varphi + H_\varphi(\rho, \varphi, z)\cos\varphi \tag{42}$$
$$H_z(x, y, z) = H_z(\rho, \varphi, z) \tag{43}$$

with $\rho = \sqrt{x^2 + y^2}$ and $\varphi = \arctan(x/y)$.

Solving explicitly the relation (40) for all combinations of i and j yields the final result in a compact form:

$$N^P_{ij}(\rho, \varphi, z) = \delta_{i3}\delta_{j3} \frac{M(\rho, \varphi, z)}{M} + \sum_{k=0}^{2} \bar{\alpha}^k_{ij}(\varphi)\{L_k(+) - L_k(-)\} \tag{44}$$

with the matrices $\bar{\alpha}^k_{ij}$ defined as:

$$\bar{\alpha}^0_{ij}(\varphi) = \frac{1}{4}\begin{pmatrix} 1 & 0 & 0 \\ 0 & 1 & 0 \\ 0 & 0 & -2 \end{pmatrix} \quad \bar{\alpha}^1_{ij}(\varphi) = \frac{1}{2}\begin{pmatrix} 0 & 0 & \cos\varphi \\ 0 & 0 & \sin\varphi \\ \cos\varphi & \sin\varphi & 0 \end{pmatrix}$$
$$\bar{\alpha}^2_{ij}(\varphi) = \frac{1}{4}\begin{pmatrix} -\cos 2\varphi & -\sin 2\varphi & 0 \\ -\sin 2\varphi & \cos 2\varphi & 0 \\ 0 & 0 & 0 \end{pmatrix} \tag{45}$$

and the auxiliary functions L_i defined as:

$$L_0(\pm) = \frac{\beta_\pm}{\pi}(\mathcal{K}_\pm - \gamma\mathcal{P}_\pm) \tag{46}$$
$$L_1(\pm) = -\frac{R\alpha_\pm}{\pi}\left(\mathcal{K}_\pm - \frac{2}{1 - k_\pm^2}(\mathcal{K}_\pm - \mathcal{E}_\pm)\right) \tag{47}$$
$$L_2(\pm) = \frac{\beta_\pm}{\pi\rho^2}\left(-\frac{1}{\alpha_\pm^2}\mathcal{E}_\pm + (\xi_\pm^2 + \rho^2 + 2R^2)\mathcal{K}_\pm + \gamma R^2\ \mathcal{P}_\pm\right) \tag{48}$$

It can be shown that such a tensor is symmetric and possesses unitary trace, in agreement with the general properties of the demagnetization tensor outlined in the previous section. The solution (44) is equivalent to that reported by [19], which corrects the solution by [17]. As an example the equivalence of the term N_{xx} is provided in the Appendix B.

6.3. The magnetometric demagnetization tensor

By inserting the relations (40) in Eq. (37) the elements of the tensor $\mathbf{N}^M$ can be obtained. The actual calculation require the evaluation of the volume integrals of the point-function demagnetization tensor, that is:

$$N^M_{ij} = \frac{1}{V}\int_V dV\, N^P_{ij} = \frac{1}{V}\int_{-L}^{+L} dz \int_0^{2\pi} d\varphi \int_0^R d\rho\, \rho N^P_{ij}(\rho, \varphi, z) \tag{49}$$

expressing the integral in cylindrical coordinates. It is trivial to show that, by performing the angular integration, all the terms depending on $\bar{\alpha}^1_{ij}(\varphi)$ and $\bar{\alpha}^2_{ij}(\varphi)$ vanish. This leaves us with only the diagonal terms in the form:

$$N^M_{ii} = \delta_{i3} + \frac{2\pi}{V}\int_{-L}^{+L} dz \int_0^R d\rho\, \rho\{\bar{\alpha}^0_{ii}\{L_0(+) - L_0(-)\}\} \tag{50}$$

The integral over L_0 is solved explicitly in the Appendix C. Here we report the final result:

$$\int_V dV\,(L_0(+) - L_0(-)) = 2V - 4\pi R^2\left\{\frac{4R}{3\pi}\left(1 - \frac{1}{m^3}[(1 - m^2)\mathcal{K}(m) - (1 - 2m^2)\mathcal{E}(m)]\right) + L\right\} \tag{51}$$

with $m = \frac{R^2}{R^2 + L^2}$. Inserting this result into the previous equation we arrive at the final exact result for the magnetometric demagnetization tensor:

$$N^M_{ii} = \delta_{i3} + 2\bar{\alpha}^0_{ii}\left(1 - \frac{R}{L}\left\{\frac{4R}{3\pi}\left(1 - \frac{1}{m^3}[(1 - m^2)\mathcal{K}(m) - (1 - 2m^2)\mathcal{E}(m)]\right) + L\right\}\right) \tag{52}$$

The diagonal of the tensor (that is, the only non-zero elements) gives the three demagnetization factors for a uniformly magnetized cylinder. The solution is equivalent to that of Tandon et al. [17] and proves the complete equivalence between the real space route adopted in this study and the Fourier space approach used by Tandon et al.

7. Numerical validation

The validity of our analytical approach is tested by comparison with numerical calculations via F.E.M. analysis (performed with MagNet 7.5, Infolytica Corporation). As a first case we consider a single, permanently magnetized cylinder, aligned with the symmetry axis along the z-axis of a Cartesian coordinate system. The cylinder has a radius of $R = 0.3$ m and semi-length $L = 6.0$ m. Note that due to the nature of the software, object dimensions must have units, but this is not expected to influence the qualitative

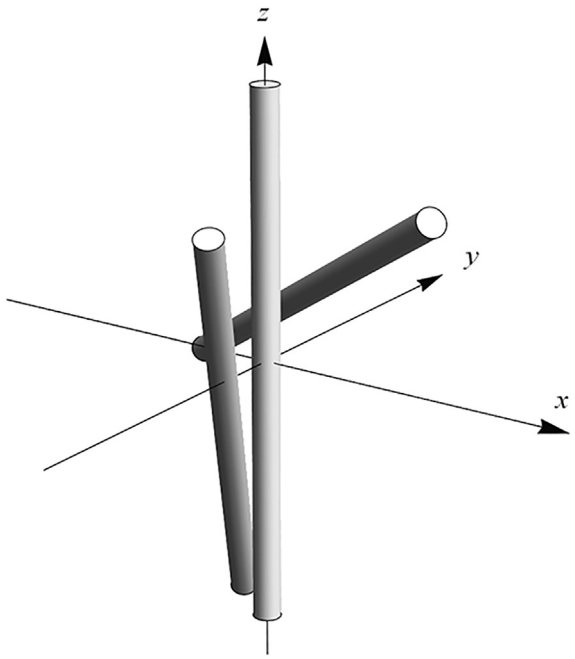

Fig. 3. Relative configuration of the three cylinder case. The permanent magnetization direction for the three unrotated cylinders is identical.

magnetic behaviour of the object. Its material properties are set to represent an ideal permanent magnet with a fixed magnetization direction and a magnitude (scalar coercivity as defined in Magnet) of 800,000 A m^{-1}, in order to generate a B-field of approximately 1T. For the single cylinder, three magnetization directions are considered: completely longitudinal, completely transversal, and a combination of two orthogonal vector components with magnetization vector $\mathbf{M} = (1/\sqrt{2}, 1/\sqrt{2}, 0)$. As a second case, a set of three cylinders with different orientations and positions is considered (see Fig. 3). The permanent magnetization direction in each cylinder is equal to $\mathbf{M} = (1/\sqrt{2}, 1/\sqrt{2}, 0)$ in the local frame of reference of the cylinder.

The magnetic field is calculated using the built-in solver of MagNet, ensuring that the calculation mesh in the vicinity of the cylinder surface(s) is sufficiently fine-grained. The field components B_x, B_y and B_z are sampled on the three perpendicular Cartesian planes through the origin, with 50 sample points per unit length along each axis. The field is also calculated for all sampled points using our analytical model. The correlation between the values from the analytical and numerical model is determined for each case by plotting the numerical values against the analytical values, and by calculating the coefficient of determination R^2, using the Pearson product-moment correlation [45].

As an example result, the comparison for the three cylinders case measured across the xy-plane is shown in Fig. 4. The agreement between the analytical model and the numerical results is good (in all cases $R^2 > 0.99$), confirming that the superposition of multiple object fields through the combination of transverse and longitudinal magnetization components gives correct results. Any noise is due to the mesh-based approach of the finite-element solver, giving rise to artefacts near the edge of the cylinder, where there is a discontinuity in the field.

8. Conclusions and outlook

We have derived an analytical expression for the magnetic field of a transversely magnetized cylinder of finite length, as an addition to the known expression for longitudinal magnetization. The formulation in terms of elliptic integrals allows for the evaluation of the field strength at any desired field point, except exactly on a surface edge. Combining both expressions allows the calculation of the magnetic field of a cylinder with an arbitrary magnetization vector.

A comparison has been made between the analytical expression and finite-element numerical calculations for magnetized cylinders. Our results are in good agreement with finite-element calculations, and provide a mesh-less solution without artefacts.

It is also possible to calculate the gradient of the magnetic field analytically. This is especially convenient for applications where magnetic forces on magnetic dipoles need to be calculated, for example in the simulation of the movement of magnetic (nano) particles in a field gradient.

Acknowledgment

Remie Janssen is thanked for critically reading the manuscript.

Appendix A. Rewriting the generalized elliptic integral

Derby and Olbert [27] provide an expression for the magnetic field of a longitudinally magnetized cylinder (equivalently, an ideal solenoid of finite length) in terms of a generalized complete elliptic integral, $C(k_c, p, c, s)$. This integral is evaluated numerically by an efficient computational procedure [38]. We find it useful to express C in the more commonly used complete elliptic integrals of the first, second and third kind to obtain expressions similar to Eq. (21). The generalized complete elliptic integral is defined in Derby and Olbert [27] as

$$C(k_c, p, c, s) = \int_0^{\pi/2} \mathrm{d}\varphi \, \frac{c\cos^2\varphi + s\sin^2\varphi}{\sqrt{\cos^2\varphi + k_c^2\sin^2\varphi}\left(\cos^2\varphi + p\sin^2\varphi\right)} \tag{A.1}$$

For the evaluation of $B_\rho, C(k_\pm, 1, 1, -1)$, is required, simplifying Eq. (A.1) to

$$\int_0^{\pi/2} \mathrm{d}\varphi \, \frac{\cos^2\varphi - \sin^2\varphi}{\sqrt{\cos^2\varphi + k_\pm^2\sin^2\varphi}\left(\cos^2\varphi + \sin^2\varphi\right)} \tag{A.2}$$

We now make a change in variable $\sin\varphi = x$, and rewrite to obtain,

$$\begin{aligned}\int_0^1 \frac{\mathrm{d}x}{\sqrt{1-x^2}} \frac{(1-x^2) - x^2}{\sqrt{(1-x^2) + k_\pm^2 x^2((1-x^2) + x^2)}} &= \int_0^1 \mathrm{d}x \, \frac{1}{\sqrt{(1-x^2)\left(1 - \left(1-k_\pm^2\right)x^2\right)}} \\ &\quad - 2\int_0^1 \mathrm{d}x \, \frac{x^2}{\sqrt{(1-x^2)\left(1 - \left(1-k_\pm^2\right)x^2\right)}}\end{aligned} \tag{A.3}$$

These integrals can be solved immediately using tabulated functions [39] (eq. 8.112). This gives finally,

$$C(k_\pm, 1, 1, -1) = \mathcal{K} - 2\left(1 - k_\pm^2\right)^{-1}(\mathcal{K} - \mathcal{E}) \tag{A.4}$$

Where the usual substitutions have been made (see Eq. (6)). This result is used in Eq. (4) as $P_1(k)$.

For the evaluation of B_z, $C(k_\pm, \gamma^2, 1, \gamma)$ is needed,[2] resulting in

[2] The fourth argument in the expression for C changes sign here with respect to the corresponding expression in Derby and Olbert [27], because of our change of sign of γ.

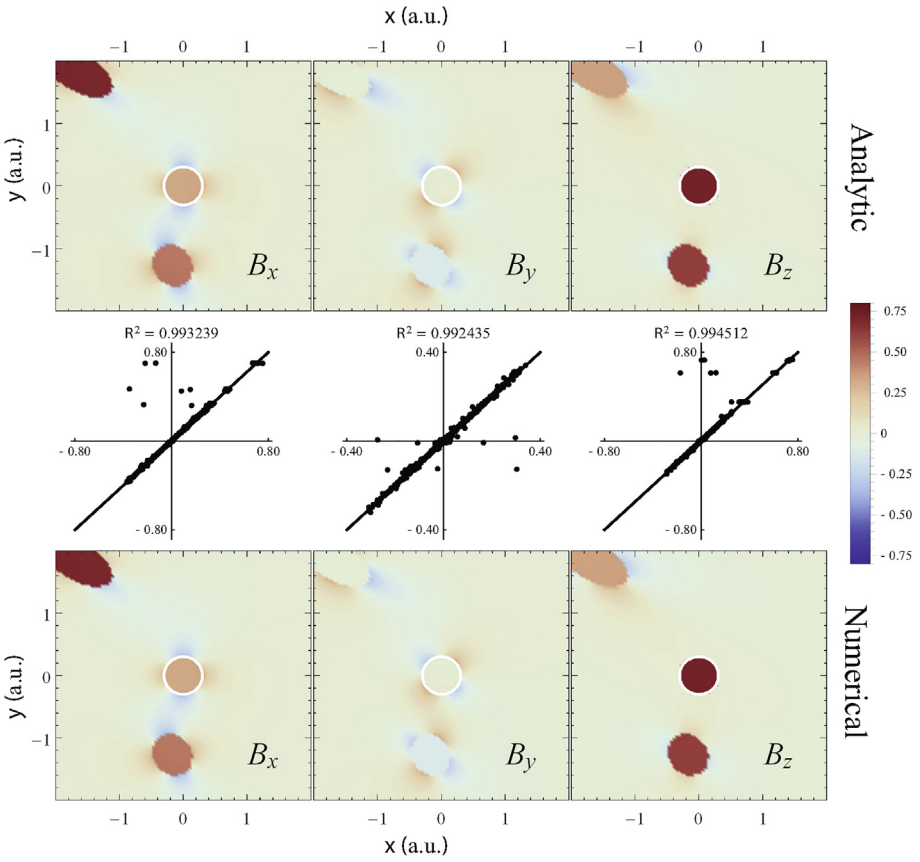

Fig. 4. Comparison of the analytical model and numerical calculations of the magnetic field (in T) sampled at the *xy*-plane for a configuration of three cylinders (see Fig. 3). The top row shows our analytical calculations and the bottom row shows the results from the finite-element calculations in MagNet. The good agreement between the two is visible from the correlation plots in the middle row.

$$\int_0^{\pi/2} \mathrm{d}\varphi \, \frac{\cos^2\varphi + \gamma \sin^2\varphi}{\sqrt{\cos^2\varphi + k_\pm^2 \sin^2\varphi}\left(\cos^2\varphi + \gamma^2 \sin^2\varphi\right)} \tag{A.5}$$

Following as before gives,

$$\begin{aligned}
&\int_0^1 \frac{\mathrm{d}x}{\sqrt{1-x^2}} \frac{(1-x^2) - \gamma x^2}{\sqrt{(1-x^2) + k_\pm^2 x^2((1-x^2) + \gamma^2 x^2)}} \\
&= \int_0^1 \mathrm{d}x \frac{1}{\sqrt{(1-x^2)\left(1 - \left(1-k_\pm^2\right)x^2\right)}(1-(1-\gamma^2)x^2)} \\
&\quad - (1+\gamma)\int_0^1 \mathrm{d}x \frac{x^2}{\sqrt{(1-x^2)\left(1 - \left(1-k_\pm^2\right)x^2\right)}(1-(1-\gamma^2)x^2)}
\end{aligned} \tag{A.6}$$

Evaluating these integrals leads to the final result, which is used in Eq. (4) as $P_2(k)$.

$$\begin{aligned}
C(k_\pm, \gamma^2, 1, \gamma) &= \mathcal{P} - (1+\gamma)\frac{1}{1-\gamma^2}(\mathcal{P} - \mathcal{K}) \\
&= \frac{1-\gamma^2}{1-\gamma^2}\mathcal{P} - \frac{1}{1-\gamma^2}(\mathcal{P} - \mathcal{K}) - \frac{\gamma}{1-\gamma^2}(\mathcal{P} - \mathcal{K}) \\
&= -\frac{1}{1-\gamma^2}(\gamma^2\mathcal{P} - \mathcal{K}) - \frac{\gamma}{1-\gamma^2}(\mathcal{P} - \mathcal{K})
\end{aligned} \tag{A.7}$$

Note that in all cases, the evaluation of the integral at $\gamma = \pm 1$ (i.e. evaluation at $\rho = R$) leads to division by zero, so that the field on the surface of the cylinder cannot be probed by these formulas.

Appendix B. Equivalence of N^P_{xx} with that of Ref. [19]

Let us first rewrite the main result from Lang [19], Eq. (36):

$$\begin{aligned}
N^P_{ij}(\rho,\varphi,z) &= \delta_{i3}\delta_{j3} D(\rho,\varphi,z) \\
&+ \sum_{\mu=0}^{2} \bar{\alpha}^\mu_{ij}(\varphi) \begin{cases} \epsilon^-_{ij}(I_\mu(\rho,\xi'_-) - I_\mu(\rho,\xi'_+)) & z > L \\ \epsilon^-_{ij}(I_\mu(\rho,0) - I_\mu(\rho,\xi'_+)) + \epsilon^+_{ij}(I_\mu(\rho,0) - I_\mu(\rho,\xi'_-)) & |z| < L \\ \epsilon^+_{ij}(I_\mu(\rho,\xi'_+) - I_\mu(\rho,\xi'_-)) & z < -L \end{cases}
\end{aligned} \tag{B.1}$$

with $\xi'_\pm = |z \pm L|$ and $D(\rho,\varphi,z)$, $\bar{\alpha}_{ij}(\varphi)$ and $\epsilon^\pm_{ij}$ as defined in [19] Eqs. (35) and (25). The terms I_μ are integrals of the Lipschitz -Hankel type:

$$I_\mu(\rho,\alpha) = \int_0^\infty dK J_1(K) J_\mu(K\rho/R) e^{-\alpha K} \tag{B.2}$$

where J_i are the Bessel functions of the first kind. Solving the summation for the specific case $i = 1, j = 1$ gives:

$$N^P_{xx} = \frac{1}{4}(\{\mu = 0\} - \cos 2\varphi \{\mu = 2\}) \tag{B.3}$$

where the terms $\{\ldots\}$ are a contraction for the corresponding terms in the summation in Eq. (B.1).

The integral $I_0(\rho, \xi'_\pm)$ solves to (Eq. (38) in [19]):

$$I_0(\rho,\xi'_\pm)=\begin{cases}-\frac{\xi'_\pm\sqrt{1-k_\pm^2}}{2\pi\sqrt{\rho R}}\mathcal{K}_\pm-\frac{1}{2}\Lambda_0(\beta'_\pm,\kappa_\pm)+1 & \rho<R\\ -\frac{\xi'_\pm\sqrt{1-k_\pm^2}}{2\pi\sqrt{\rho R}}+\frac{1}{2} & \rho=R\\ -\frac{\xi'_\pm\sqrt{1-k_\pm^2}}{2\pi R\sqrt{\rho R}}\mathcal{K}_\pm+\frac{1}{2}\Lambda_0(\beta'_\pm,\kappa_\pm) & \rho>R\end{cases}\tag{B.4}$$

with $\sin^2(\kappa_\pm)=\frac{4R\rho}{(\rho+R)^2+\xi_\pm^2}$ and $\beta'_\pm=\arcsin(\alpha_\pm\xi_\pm,\kappa_\pm)$ and $\Lambda_0(\beta'_\pm,\kappa_\pm)$ is Heuman's Lambda Function as defined in [46]. The integral $I_2(\rho,\xi'_\pm)$ solves to (Eq. (44) in [19]):

$$I_2(\rho,\xi'_\pm)=\begin{cases}\frac{2\sqrt{R}\xi'_\pm}{\pi\sqrt{1-k_\pm^2}\rho^{3/2}}\mathcal{E}_\pm-\frac{\xi'_\pm\sqrt{1-k_\pm^2}(\xi_\pm^2+\rho^2+2R^2)}{2\pi\sqrt{R}\rho^{5/2}}\mathcal{K}_\pm-\frac{R^2}{2\rho^2}\Lambda_0(\beta'_\pm,\kappa_\pm)+\frac{R^2}{\rho^2} & \rho>R\\ \frac{2\sqrt{R}\xi'_\pm}{\pi\sqrt{1-k_\pm^2}\rho^{3/2}}\mathcal{E}_\pm-\frac{\xi'_\pm\sqrt{1-k_\pm^2}(\xi_\pm^2+\rho^2+2R^2)}{2\pi\sqrt{R}\rho^{5/2}}\mathcal{K}_\pm-\frac{R^2}{2\rho^2} & \rho=R\\ \frac{2\sqrt{R}\xi'_\pm}{\pi\sqrt{1-k_\pm^2}\rho^{3/2}}\mathcal{E}_\pm-\frac{\xi'_\pm\sqrt{1-k_\pm^2}(\xi_\pm^2+\rho^2+2R^2)}{2\pi\sqrt{R}\rho^{5/2}}\mathcal{K}_\pm+\frac{R^2}{2\rho^2}\Lambda_0(\beta'_\pm,\kappa_\pm) & \rho<R\end{cases}\tag{B.5}$$

By switching $\xi'_\pm$ for $\xi_\pm$ as defined earlier (that is, explicitly writing the absolute value) and using the results $\Lambda_0(0,x)=0$ and $\Lambda_0(\pi/2,x)=1$ (which can be easily proven using the definition of Heuman's Lambda and the Legendre Relation for elliptic integrals), it is possible to greatly simplify all the cumbersome cases for ρ and z in Eqs. (B.4), (B.5) and (B.1) to a single, more elegant result:

$$N_{xx}^P=\frac{1}{4}(\{L_0(+)-L_0(-)\}-\cos 2\varphi\,\{L_2(+)-L_2(-)\})\tag{B.6}$$

with:

$$L_0(\pm)=\frac{\xi_\pm\sqrt{1-k_\pm^2}}{2\pi\sqrt{\rho R}}\mathcal{K}_\pm-\frac{\gamma}{2|\gamma|}\Lambda_0(\beta'_\pm,\kappa_\pm)\tag{B.7}$$

$$L_2(\pm)=-\frac{2\sqrt{R}\xi_\pm}{\pi\sqrt{1-k_\pm^2}\rho^{3/2}}\mathcal{E}_\pm+\frac{\xi_\pm\sqrt{1-k_\pm^2}(\xi_\pm^2+\rho^2+2R^2)}{2\pi\sqrt{R}\rho^{5/2}}\mathcal{K}_\pm+\frac{\gamma R^2}{2|\gamma|\rho^2}\Lambda_0(\beta'_\pm,\kappa_\pm)\tag{B.8}$$

Lastly, Heuman's Lambda function can be expressed in terms of complete elliptic integrals [47]:

$$\Lambda_0(\beta'_\pm,\kappa_\pm)=\frac{2|\gamma|}{\pi}\xi_\pm\alpha_\pm\mathcal{P}_\pm\tag{B.9}$$

This leads to the final result for the auxiliary functions L_i after some refactoring:

$$L_0(\pm)=\frac{\beta_\pm}{\pi}(\mathcal{K}_\pm-\gamma\mathcal{P}_\pm)\tag{B.10}$$

$$L_2(\pm)=\frac{\beta_\pm}{\pi\rho^2}\left(-\frac{1}{\alpha_\pm^2}\mathcal{E}_\pm+(\xi_\pm^2+\rho^2+2R^2)\mathcal{K}_\pm+\gamma R^2\ \mathcal{P}_\pm\right)\tag{B.11}$$

Now we explicitly solve for the first relation in 40:

$$\begin{aligned}\acute{N}_{xx}^P&=-\frac{1}{M}H_x=\frac{1}{M}(H_\rho\cos\varphi-H_\varphi\sin\varphi)\\&=-\frac{R}{2\pi\rho}\{\beta_+(P_4(k_+)\cos\varphi^2-2P_3(k_+)\sin\varphi^2)\\&\quad-\beta_-(P_4(k_-)\cos\varphi^2-2P_3(k_-)\sin\varphi^2)\}\end{aligned}\tag{B.12}$$

where $\acute{N}_{xx}^P$ indicates the derivation according to our field expressions. Upon explicitly writing the auxiliary functions P_3 and P_4, the following result follows:

$$\begin{aligned}\acute{N}_{xx}^P&=\frac{1}{4\pi}\{\beta_+(\mathcal{K}_+-\gamma\mathcal{P}_+)-\beta_-(\mathcal{K}_--\gamma\mathcal{P}_-)\}\\&\quad+\frac{\cos 2\varphi}{4\pi\rho^2}\left\{\beta_+\left(\frac{\mathcal{E}_+}{\alpha_+^2}-(\xi_+^2+\rho^2+2R^2)\mathcal{K}_+-\gamma R^2\mathcal{P}_+\right)\right.\\&\quad\left.-\beta_-\left(\frac{\mathcal{E}_-}{\alpha_-^2}-(\xi_-^2+\rho^2+2R^2)\mathcal{K}_--\gamma R^2\mathcal{P}_-\right)\right\}\end{aligned}\tag{B.13}$$

It is trivial to show that this expression is equivalent to N_{xx} as derived above. The demonstration can be extended to all the other tensor components, thus giving complete equivalence between the formulations.

Appendix C. Integral of $L_0(\pm)$

The integral to be solved is the following:

$$\int_V dV\,(L_0(+)-L_0(-))\tag{C.1}$$

Before starting we write some useful relations and identities [46,48]

$$\left(\frac{1}{x}\frac{d}{dx}\right)^k\{x^iJ_i(x)\}=x^{i-k}J_{i-k}(x)\tag{C.2}$$

$$\int_0^\infty dx\,e^{-px}J_1(ax)J_0(bx)=-\frac{pk}{2\pi a\sqrt{ab}}\left(\mathcal{K}(k)-\frac{b-a}{b+a}\mathcal{P}(k,g)\right)+\frac{1}{a}\tag{C.3}$$

$$\int_0^\infty dx\,e^{-2px}\frac{J_1^2(ax)}{x^2}=\frac{4a}{3\pi m^3}\left((1-m^2)\mathcal{K}(m)-(1-2m^2)\mathcal{E}(m)\right)-p\tag{C.4}$$

where J_i are the Bessel's Functions of the First Kind and $k^2=\frac{4ab}{p^2+(a+b)^2}$ $m=\frac{a^2}{p^2+a^2}$ and $g=\frac{2ab}{(a+b)^2}$. Furthermore, $(a,b,p\geqslant 0)$ and $(a>b)$.

We start by expanding the auxiliary function L_0 in the integral C.1:

$$\begin{aligned}\int_V dV\,(L_0(+)-L_0(-))&=\int_V dV\frac{1}{\pi}(\beta_+(\mathcal{K}_+-\gamma\mathcal{P}_+)-\beta_-(\mathcal{K}_--\gamma\mathcal{P}_-))\\&=\int_{-L}^{+L}dz\int_0^{2\pi}d\varphi\int_0^R d\rho\,\frac{\rho}{2\pi\sqrt{R\rho}}\{k_+(z-L)(\mathcal{K}_+-\gamma\mathcal{P}_+)\\&\quad+k_-(L-z)(\mathcal{K}_--\gamma\mathcal{P}_-)\}\end{aligned}\tag{C.5}$$

where we made use of the definition of $\beta_\pm$ and inverted the sign for the negative term. It is now possible to use C.3 and the definition $\gamma=\frac{\rho-R}{\rho+R}$ to rewrite the result, arriving to the expression:

$$\int_{-L}^{+L}dz\int_0^{2\pi}d\varphi\int_0^R d\rho\,R\rho\left\{\frac{2}{R}-\int_0^\infty dx\,(e^{-p_+x}+e^{-p_-x})J_1(Rx)J_0(\rho x)\right\}\tag{C.6}$$

where $p_\pm=L\pm z$. In the limits of integration, $p_\pm\geqslant 0$ and thus the use of (C.2) is justified. By solving for the unity terms and rearranging the integral order, we arrive to:

$$\begin{aligned}&2V-2\pi R\int_{-L}^{+L}dz\int_0^\infty dx\,(e^{-p_+x}+e^{-p_-x})J_1(Rx)\int_0^R d\rho\,\rho J_0(\rho x)\\&=2V-2\pi R\int_{-L}^{+L}dz\int_0^\infty dx\,(e^{-p_+x}+e^{-p_-x})\frac{J_1(Rx)}{x}\\&\quad\times\int_0^R d\rho\,\frac{d}{d(\rho x)}(\rho xJ_1(\rho x))=2V-2\pi R^2\\&\quad\times\int_{-L}^{+L}dz\int_0^\infty dx\,(e^{-p_+x}+e^{-p_-x})\frac{J_1(Rx)^2}{x}\end{aligned}\tag{C.7}$$

where we have used (C.2) in the second passage. We can again change the integration order to have:

$$\begin{aligned}&2V-2\pi R^2\int_0^\infty dx\frac{J_1(Rx)^2}{x}\int_{-L}^{+L}dz\,(e^{-p_+x}+e^{-p_-x})\\&=2V-4\pi R^2\int_0^\infty dx\frac{J_1(Rx)^2}{x}\int_0^{2L}dz'\,(e^{-z'x})\\&=2V-4\pi R^2\int_0^\infty dx\frac{J_1(Rx)^2}{x^2}(1-e^{-2Lx})\end{aligned}\tag{C.8}$$

where in the second passage we applied a change of variable $z' = L \pm z$ to reduce the two exponentials to a single term. The resulting integral can be split as:

$$2V - 4\pi R^2 \left\{ R \int_0^\infty dx' \frac{J_1(x')^2}{x'^2} - \int_0^\infty dx\, e^{-2Lx} \frac{J_1(Rx)^2}{x^2} \right\} \tag{C.9}$$

Both the terms can be separately expressed in terms of C.4, yielding the final result (with $m = \frac{R^2}{L^2+R^2}$):

$$\int_V dV\,(L_0(+) - L_0(-)) = 2V - 4\pi R^2 \left\{ \frac{4R}{3\pi} \left(1 - \frac{1}{m^3} \left[(1-m^2)\mathcal{K}(m) - (1-2m^2)\mathcal{E}(m) \right] \right) + L \right\} \tag{C.10}$$

Appendix D. Supplementary data

Supplementary data associated with this article can be found, in the online version, athttps://doi.org/10.1016/j.jmmm.2018.02.003.

References

[1] J.C. Maxwell, A treatise on electricity and magnetism, Oxford University Press Clarendon, First published 1873, Oxford, 1955.
[2] J. Stratton, Electromagnetic Theory, McGraw-Hill Book Company, New York and London, 1941.
[3] J. Jackson, Classical Electrodynamics, third ed., Wiley, New York, NY, 1999.
[4] D. Griffiths, Introduction to Electrodynamics, Prentice-Hall Inc, New Jersey, 1999.
[5] J. Osborn, Demagnetization factors of the general ellipsoid, Phys. Rev. 67 (11–1) (1945) 351–357, https://doi.org/10.1103/PhysRev. 67.351.
[6] M. Beleggia, M. De Graef, Y. Millev, Demagnetization factors of the general ellipsoid: an alternative to the Maxwell approach, Philos. Mag. 86 (16) (2006) 2451–2466, https://doi.org/10.1080/14786430600617161.
[7] M. Beleggia, M. De Graef, Y. Millev, D. Goode, G. Rowlands, Demagnetization factors for elliptic cylinders, J. Phys. D: Appl. Phys. 38 (18) (2005) 3333, https://doi.org/10.1088/0022-3727/38/18/001.
[8] R. Joseph, Ballistic demagnetization factor in uniformly magnetized cylinders, J. Appl. Phys. 37 (13) (1966) 4639–4643, https://doi.org/10.1063/1.1708110.
[9] D.-X. Chen, J. Brug, R. Goldfarb, Demagnetization factors for cylinders, IEEE Trans. Magn. 27 (1991) 3601–3619, https://doi.org/10.1109/20.102932.
[10] D.-X. Chen, E. Pardo, A. Sanchez, Fluxmetric and magnetometric demagnetizing factors for cylinders, J. Magn. Magn. Mater. 306 (1) (2006) 135–146, https://doi.org/10.1016/j.jmmm.2006.02.235.
[11] A. Aharoni, Demagnetizing factors for rectangular ferromagnetic prisms, J. Appl. Phys. 83 (6) (1998) 3432–3434, https://doi.org/10.1063/1.367113.
[12] K. Metlov, Vortex precession frequency and its amplitude-dependent shift in cylindrical nanomagnets, J. Appl. Phys. 114 (22) (2013), https://doi.org/10.1063/1.4844435.
[13] K. Guslienko, K. Metlov, Evolution and stability of a magnetic vortex in a small cylindrical ferromagnetic particle under applied field, Phys. Rev. B 63 (10) (2001), https://doi.org/10.1103/PhysRevB.63.100403.
[14] K. Metlov, K. Guslienko, Quasiuniform magnetization state in soft ferromagnetic nanocylinders, Phys. Rev. B 70 (5) (2004), https://doi.org/10.1103/PhysRevB.70.052406.
[15] T. Taniguchi, Indirect excitation of self-oscillation in perpendicular ferromagnet by spin Hall effect, Appl. Phys. Lett. 111 (2) (2017), https://doi.org/10.1063/1.4991663, Supplementary Material.
[16] L. Kraus, Demagnetization tensor of a cylinder, Czech J. Phys. 23 (5) (1973) 512–519, https://doi.org/10.1007/BF01593828.
[17] S. Tandon, M. Beleggia, Y. Zhu, M. De Graef, On the computation of the demagnetization tensor for uniformly magnetized particles of arbitrary shape. Part I: Analytical approach, J. Magn. Magn. Mater. 271 (1) (2004) 9–26, https://doi.org/10.1016/j.jmmm.2003.09.011.
[18] M. Beleggia, M. De Graef, On the computation of the demagnetization tensor field for an arbitrary particle shape using a Fourier space approach, J. Magn. Magn. Mater. 263 (1–2) (2003) L1–L9, https://doi.org/10.1016/S0304-8853(03)00238-5.
[19] F. Lang, S. Blundell, Fourier space derivation of the demagnetization tensor for uniformly magnetized objects of cylindrical symmetry, J. Magn. Magn. Mater. 401 (2016) 1060–1067, https://doi.org/10.1016/j.jmmm.2015.10.133.
[20] J. Coggon, Electromagnetic and electrical modeling by the finite element method, Geophysics 36 (1971) 132–155, https://doi.org/10.1190/1.1440151.
[21] J.-M. Jin, The Finite Element Method in Electromagnetics, third ed., John Wiley & Sons, 2014.
[22] K. Warnke, Finite-element modeling of the separation of magnetic microparticles in fluid, IEEE Trans. Magn. 39 (2003) 1771–1777, https://doi.org/10.1109/TMAG.2003.810609.
[23] V. Schaller, U. Kräling, C. Rusu, K. Petersson, J. Wipenmyr, A. Krozer, G. Wahnström, A. Sanz-Velasco, P. Enoksson, C. Johansson, Motion of nanometer sized magnetic particles in a magnetic field gradient, J. Appl. Phys. 104 (2008) 093918, https://doi.org/10.1063/1.3009686.
[24] M. Garrett, Axially symmetric systems for generating and measuring magnetic fields. Part I, J. Appl. Phys. 22 (1951) 1091–1107, https://doi.org/10.1063/1.1700115.
[25] E. Callaghan, S. Maslen, The Magnetic Field of a Finite Solenoid, National Aeronautics and Space Administration, Washington, 1960, URL: < http://www.osti.gov/scitech/biblio/4121210>.
[26] J. Conway, Exact solutions for the magnetic fields of axisymmetric solenoids and current distributions, IEEE Trans. Magn. 37 (2001) 2977–2988, https://doi.org/10.1109/20.947050.
[27] N. Derby, S. Olbert, Cylindrical magnets and ideal solenoids, Am. J. Phys. 78 (2010) 229–235, https://doi.org/10.1119/1.3256157.
[28] M. Garrett, Calculation of fields, forces, and mutual inductances of current systems by elliptic integrals, J. Appl. Phys. 34 (1963) 2567–2573, https://doi.org/10.1063/1.1729771.
[29] J. Lane, R. Youngquist, C. Immer, J. Simpson, Magnetic Field, Force, and Inductance Computations for an Axially Symmetric Solenoid, National Aeronautics and Space Administration, Washington, 2001, URL: < http://ntrs.nasa.gov/search.jsp?R=20140002332>.
[30] J. Oberteuffer, Magnetic separation: a review of principles, devices, and applications, IEEE Trans. Magn. 10 (2) (1974) 223–238, https://doi.org/10.1109/TMAG.1974.1058315.
[31] G. Wysin, Demagnetization Fields, 2012, last accessed 2017, Oct 30. URL: < https://www.phys.ksu.edu/personal/wysin/notes/demag.pdf>.
[32] R. Baars, Random porous media and magnetic separation of magnetic colloids (Ph.D. thesis), Utrecht University, The Netherlands, iD: URN:NBN:NL:UI:10–1874-326013, 2016. URL: < http://dspace.library.uu.nl/handle/1874/326013>.
[33] W. Druyvesteyn, J. Dorleijn, Calculations on some periodic magnetic domain structures – consequences for bubble devices, Philips Res. Rep. 26 (1) (1971) 11+.
[34] K. Guslienko, Magnetostatic interdot coupling in two-dimensional magnetic dot arrays, Appl. Phys. Lett. 75 (3) (1999) 394–396, https://doi.org/10.1063/1.124386.
[35] K. Metlov, Micromagnetics and interaction effects in the lattice of magnetic dots, J. Magn. Magn. Mater. 215 (SI) (2000) 37–39. 14th International Symposium on Soft Magnetic Materials (SMM14), Balatonfured, Hungary, Sep 08–10, 1999. doi:10.1016/S0304-8853(00)00060-3.
[36] E. Stoner, E. Wohlfarth, A mechanism of magnetic hysteresis in heterogeneous alloys, IEEE Trans. Magn. 27 (1991) 3475–3518, https://doi.org/10.1109/TMAG.1991.1183750.
[37] Z. Nagy, B. Nelson, Lagrangian modeling of the magnetization and the magnetic torque on assembled soft-magnetic mems devices for fast computation and analysis, IEEE Trans. Rob. 28 (4) (2012) 787–797, https://doi.org/10.1109/TRO.2012.2193230.
[38] R. Bulirsch, Numerical calculation of elliptic integrals and elliptic functions, Numer. Math. 7 (1965) 78–90, https://doi.org/10.1007/BF01397975.
[39] I. Ryzhik, I. Gradstein, Tables of Series, Products and Integrals, Veb. Deutscher Verlag der Wissenschaften, 1957.
[40] B. Carlson, Computing elliptic integrals by duplication, Numer. Math. 33 (1979) 1–16, https://doi.org/10.1007/BF01396491.
[41] T. Fukushima, Precise and fast computation of the general complete elliptic integral of the second kind, Math. Comput. 80 (2011) 1725–1743, https://doi.org/10.1090/S0025-5718-2011-02455-5.
[42] T. Fukushima, Precise and fast computation of a general incomplete elliptic integral of third kind by half and double argument transformations, J. Comput. Appl. Math. 236 (2012) 1961–1975, https://doi.org/10.1016/j.cam.2011.11.007.
[43] E. Schlömann, A sum rule concerning the inhomogeneous demagnetizing field in nonellipsoidal samples, J. Appl. Phys. 33 (9) (1962) 2825–2826, https://doi.org/10.1063/1.1702557.
[44] R. Moskowitz, E. Della Torre, Theoretical aspects of demagnetization tensors, IEEE Trans. Magn. 2 (4) (1966) 739–744, https://doi.org/10.1109/TMAG.1966.1065973, URL: < http://ieeexplore.ieee.org/document/1065973/>.
[45] O. Behnke, K. Krninger, Data Analysis in High Energy Physics: A Practical Guide to Statistical Methods, Wiley, 2013.
[46] M. Abramowitz, I. Stegun, Handbook of Mathematical Functions with Formulas, Graphs, and Mathematical Tables, vol. 56, Dover Publications, 1964.
[47] T. Lemczyk, M. Yovanovich, Efficient evaluation of incomplete elliptic integrals and functions, Comput. Math. Appl. 16 (9) (1988) 747–757, https://doi.org/10.1016/0898-1221(88)90010-7.
[48] S. Okui, Complete elliptic integrals resulting from finite integrals of Bessel functions, J. Res. NBS. B Math. Sci. 78 (3) (1974) 113–135, https://doi.org/10.6028/jres.078B.018.